

Laser beam quality factor (M^2) measured by distorted fresnel zone plates

R. Cortés*, R. Villagómez, V. Coello, and R. López

CICESE Unidad Monterrey,

*Km. 9.5 Nueva Carretera al Aeropuerto, Parque de Investigación e Innovación Tecnológica (PIIT),
66629, Apodaca, N.L., México.*

Recibido el 20 de agosto de 2007; aceptado el 17 de junio de 2008

In this paper we present a novel method, based on diffractive optics, for measuring M^2 . This novel optical arrangement consists of a lens along with a set of 1 or 2 distorted diffraction gratings and a single array detector. As a result, this system produces simultaneous images of a number of different object planes centred over the laser beam propagation axis symmetrically to the laser beam waist. This image is gathered around the image plane using a CCD camera producing, in a single image and after some image processing, an instantaneous measurement for the laser beam quality. This technique allows for the possibility of monitoring the beam quality in real time, in a continuous or pulse-to-pulse mode operation. Nowadays, high power laser machining is a standard technique in manufacturing material processing that is widely used in industry. Although these lasers are not always stable for long periods of time, which is required in this kind of process, it usually takes considerable time to diagnose them and restore them to working order. The M^2 parameter is a numerical expression for laser beam quality that can be measured in real time over a process line. However, to measure the M^2 parameter, several measurements in the neighbourhood of the laser beam waist are required.

Keywords: Optical diffraction gratings; Nd:YAG laser; Beam quality.

En este artículo, presentamos un método novedoso basado en óptica difractiva para medir M^2 . Este nuevo arreglo óptico consiste de una lente con un conjunto de 1 o dos rejillas de difracción y un simple arreglo detector. Como resultado, este sistema produce imágenes simultáneas, de un número de diferentes planos-objeto centrados a lo largo del eje de propagación simétricamente a la cintura del haz láser. Estas imágenes son colectadas simultáneamente en una sola imagen mediante una cámara CCD generando en una sola imagen y después de algún procesamiento de la imagen, una medición instantánea para la calidad del haz láser. Esta técnica permite la posibilidad de monitorear en tiempo real la calidad del haz en un modo de operación continuo o pulso a pulso. Hoy en día, el maquinado con láser de alta potencia es una técnica estándar en la manufactura para el procesamiento de materiales. Aunque estos láseres no son siempre estables durante largos períodos de tiempo, el cual es requerido en esta clase de procesos, la mayoría de las veces diagnosticar y poner de nuevo a trabajar lleva un tiempo significativo. El parámetro M^2 es una expresión numérica para la calidad del haz láser que puede ser medida en tiempo real en un proceso en línea. Sin embargo para medir el parámetro M^2 , varias mediciones en la vecindad de la cintura del haz láser son requeridas.

Descriptores: Rejillas de difracción óptica; láser Nd:YAG; calidad del haz.

PACS: 42.79.Dj; 42.55.Rz; 42.60.Jf

1. Introduction

High power lasers are increasingly used in a wide range of manufacturing processes and several industrial and service sectors. They are typically applied to cutting, welding, drilling, heat treatment of materials and cleaning [1-3]. Laser machining has now become a standard manufacturing technique ranging from the use of CO₂ lasers for cutting engineering ceramics laminates [4] to the use of YAG lasers for high-precision micromachining [3]. Delivery of high power Nd:YAG laser beams through optical fibres has become established as a standard mode of operation used for material processing, and notably for welding. But, its development has been restricted by limitations in the quality and power density achievable for different processing operations [3]. Alternatively, optical properties (small core diameter, number of modes) can be used to improve the intensity distribution beam. However, these lasers are not always stable over the very long periods of time required in manufacturing processes, e.g. thermal effects in solid-state lasers materials are influenced by the absorption of pump as well as the heat flow to the cooled periphery [5]. Consequently, changes in these

properties may cause the process to fail or be unsatisfactory. Laser problems can take considerable time to diagnose and repair, especially when there is no equipment available to rapidly analyse the laser beam parameters online. In particular, there is evidence that in some industrial pulsed lasers the output beam quality varies significantly from pulse to pulse. Additional problems can also appear when a fibre optic beam delivery system is used because it might lead to some deterioration in the beam quality due to interference between the many guided modes, thus affecting the beam spatial intensity distribution [3] and curvature-induced mode-coupling process [6]. This effect leads to a loss of beam quality noticing how the ‘spot’ spreads out as the beam is guided [6-7]. For this reason, it is important to be able to monitor the laser beam on high power lasers, where the fact is that it is preferable to make these measurements in real time.

The parameter M^2 is a numerical expression for the beam quality of laser systems and it can be written as: [8]

$$M^2 = \frac{\pi w_0 \theta_0}{\lambda}, \quad (1)$$

where w_0 is the beam waist or “spot size”, and θ_0 the cone

half-angle (see Fig. 1). Noticing that M^2 equals 1, we have a perfect Gaussian beam. Higher values for M^2 means poorer quality [8] as the beam propagates a far from a perfect Gaussian beam shape. Thus, beam quality gives us a description of how well a laser beam can be focused.

In order to properly measure the M^2 parameter, it is necessary to take a series of measurements on a number of separate planes around the laser beam waist (typically ~ 10 for an accurate measurement). This can be achieved in different ways. One approach consists in using several beam splitters and array detectors placed at different points along the propagation axis. Nevertheless, this approach has its disadvantages. It is more complicated and has a low optical efficiency (mainly because of the use of many beam splitters) making such a device impractical to be improved in a real process line. A second approach consists in the use of a conventional scanning beam setup with an array detector collecting, in different places, several sequential images of the laser beam spot. Although this method is more precise, it takes a long time to take all the necessary measurements and it is not possible to do this in real time. In this work we propose the use of a novel optical setup, which is based on a diffractive optical element that consists of a grating structure. The proposed setup incorporates beam splitter properties giving, as a result, a distorted diffraction grating with the capacity to produce simultaneous images of multiple object planes over a single image plane where the CCD detector is placed.

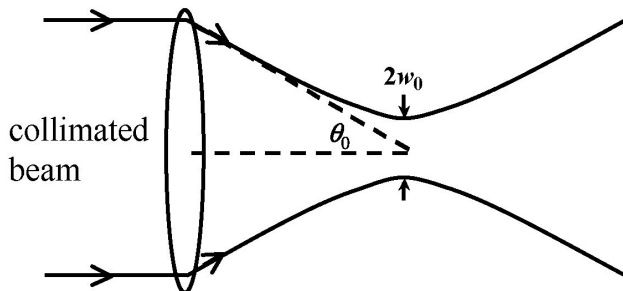


FIGURE 1. Concept of M^2 used to characterize the laser beam quality.

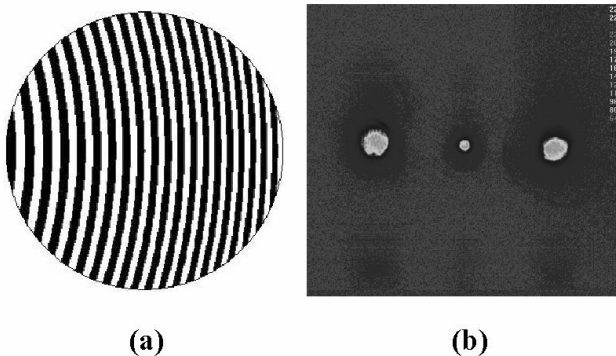


FIGURE 2. (a) Diffraction grating with distortion of $W_{20} = 3\lambda$ (b) Beam collimated split by distorted diffraction grating with $W_{20} = 84\lambda$.

Essentially, this device uses a lens close to 1 or 2 distorted diffraction gratings and a single array detector. This novel arrangement can provide an instantaneous measurement of the beam quality. Beam quality can hence be monitored in a continuous or pulse-to-pulse mode operation.

2. System design

This measurement technique applied to the evaluation of the beam quality in high power lasers is based in the use of diffraction gratings with grating lines distorted. An example of such distorted diffraction grating is shown in Fig. 2. Its design is described in UK patent application GB 980499.68 and previous publications [9,10]. The distorted diffraction grating becomes off-axis Fresnel zone plate lenses. The effect is produced by arcs of circles off-axis centred. The distorted diffraction grating is a binary phase grating. The dark regions represent areas that have an increased optical thickness of slightly less than $\lambda/2$, as indicated in Fig. 2. In this case, the optical efficiency for each diffracted order can be adjusted by changing the height of the step profile. In the simplest arrangement, a single grating is used. The grating with lines distorted quadratically has a focusing power in the non-zero orders according to [9]:

$$f_g = \frac{R^2}{2mW_{20}}, \quad (2)$$

where m is the diffraction order, W_{20} is the standard defocusing power (+1 order) and R is the radius of the grating aperture. Therefore, this distorted grating works as a set of lenses with negative, neutral and positive power. The focusing power in the non-zero orders was calculated considering the phase profile that generates a spherical wave front in the paraxial approximation. In this case, defocusing is regarded as a phase shift varying with the distance from the optical axis, relative to the in-focus system. The accuracy of the grating alignment and aberrations effects are discussed by Blanchard *et al.* [11].

In practice, it is more useful to use a grating in close proximity to a lens in order to modify its focal length for each diffracted order, as indicated in Fig. 2. This grating-lens combination gives as a result the superposition of three object planes onto a single image plane with the +1 and -1 orders laterally shifted. The zero order is arranged to stay by the propagation axis (see Fig. 3). If the CCD camera is placed at the geometrical focal point of the lens, the zero order diffraction generates an image of the beam waist when a collimated beam enters the system. The +1 and -1 orders, meanwhile, provide images of the beam corresponding to planes after and before the focal plane. Consequently, we have 3 spots of the laser beam in the same image plane, which is sufficient to proceed to fit the quality of the collimated laser beam. Moreover, one has to take into consideration that, the distorted grating introduces a magnification that is associated with the

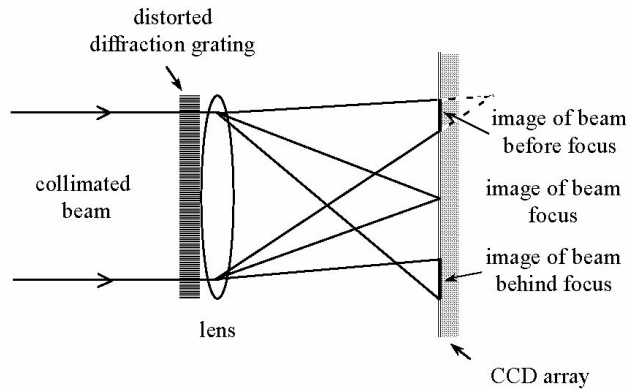


FIGURE 3. Beam quality measurement system using a single distorted grating.

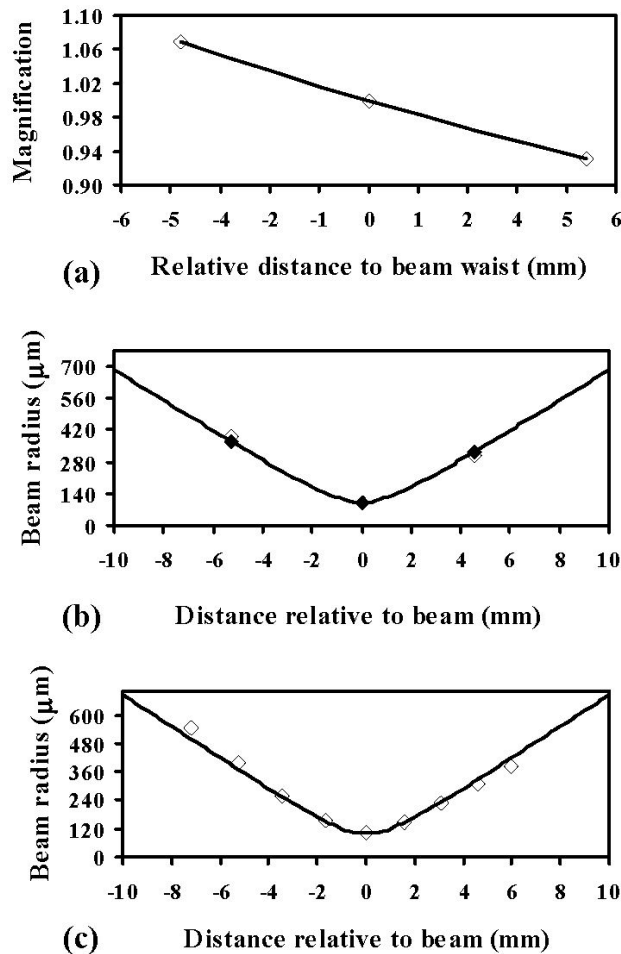


FIGURE 4. Reconstruction of beam distribution from diffracted spot beam size. Lasers parameters: $w_o = 100 \mu\text{m}$, $\lambda = 1064 \text{ nm}$, $M^2 = 30$: (a) Diamond mark for first grating with $W_{20} = 14\lambda$ and triangle mark for second grating with $W_{20} = 42\lambda$.

image in the m th diffraction order, M_m , [9] given by:

$$M_m = M_0 + \frac{2mvW_{20}}{R^2}, \quad (3)$$

where M_0 is the magnification of the image associated with the zero order and ν is the image distance for zero order.

The overall performance of the distorted diffraction grating is its effectiveness in having simultaneously images matching, or overlapping, different object planes of the beam onto a single image plane used to measure M^2 . Therefore, when the camera is placed in the image plane, corresponding to the zero order, the grating generates side-by-side simultaneous images of the three different object planes, collecting them in the detector plane.

3. Numerical simulation

In order to fit our experimental measurement to the best value of the M^2 parameter, we start by simulating our experiment as follows. A wavelength of 1064 nm was used for a laser beam with a beam quality $M^2 = 20$. The grating parameters used in these calculations had a distortion of $W_{20} = 57\lambda$, an aperture radius of 11 mm, a period of $44 \mu\text{m}$ at the aperture centre, and a lens with a focal length of 70 mm. The real beam size of each spot diffracted is recovered from the magnification introduced by the distorted grating, as shown in Fig. 4a. The proposal simulation is then compared with the standard conventional technique (continuous line) as indicated in Fig. 4b. In this figure, the white diamond marks represent the spot size for the diffracted order while the black diamond marks represent the same points after being processed. Here, the magnification factor is taken into account for each diffracted order. According to Eq. (2), the separation between object planes is a function of the grating parameters and the focal length of the lens close to the grating. On the other hand, a more accurate measurement can be made when a second grating is introduced into the system. In this case, this second grating is aligned orthogonally to the first, which is designed to give an effective object spacing of one-third of the first grating, consequently increasing the number of planes overlapping in the image plane of the entire system. This result is due to the effect of splitting each image created by the first beam into 3 (-1, 0 and +1), and the second grating takes these three spots as objects to produce three times three image spots into the image plane after passing the focusing lens. In our numerical simulation, we simulate two gratings, with the second grating having a focal length one-third that of the first grating. The spots diffracted for these two crossed gratings are shown in Fig. 4c.

4. Experimental and results

As we mentioned earlier, the technique we developed for monitoring the beam quality in high power lasers uses a cross-distorted diffraction grating in close proximity to a lens, as shown in Fig. 3. The grating period d_o at the center of the mask is associated with the transverse separation between images through the Bragg diffraction equation. In our case, a suitable lens was used in close approximation with the gra-

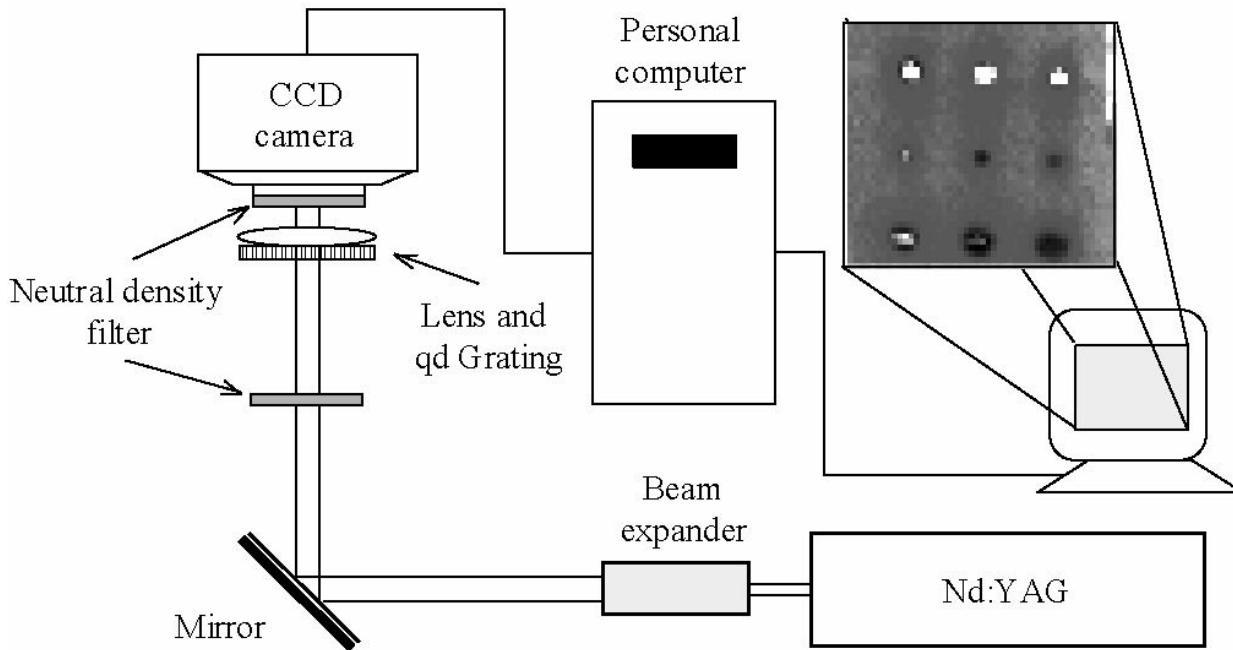


FIGURE 5. Magnification of each grating: Diamond mark grating with $W_{20} = 14\lambda$ and triangle mark for second grating with $W_{20} = 42\lambda$.

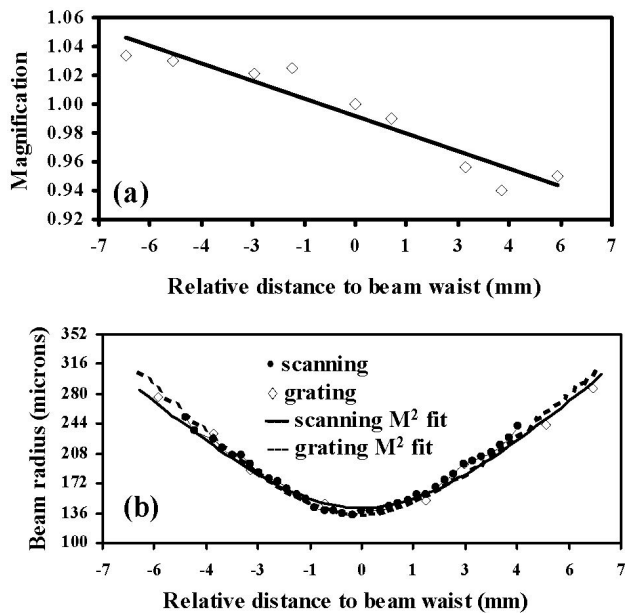


FIGURE 6. (a) Magnification of the two grating-lens system. (b) Example of beam quality measurement employing two gratings and by scanning.

ting. Non-linear effects are not considered due to the low intensity level. The performance of our entire optical setup system was tested on a typical high power laser (GSI Lumonics JK702) measuring the M^2 . The experimental setup is shown in Fig. 5. Light from the pulsed Nd:YAG laser is collimated by the beam expander (10X) and reflected by a mirror delivering the laser beam to the grating-lens combination setup. As the beam crosses this setup, the beam is diffracted by the quadratically distorted (qd) grating having different

levels of focusing power for each diffracted order. The output beam leaving the qd grating-lens is imaged onto a screen CCD camera, (COHU, model 4915) placed at a distance to image the zero diffracted order. The use of neutral density filters has two functions: to avoid saturation on the CCD and to eliminate external noise that can affect the images. Measurements were performed in continuous mode. The beam diameter was obtained using commercially available beam profiling package software (*Spiricon LBA-300 PC*), based on the second moment beam width definition. The experimental results obtained using a two grating-lens combination are shown in Fig. 6. The experimental magnification for this system is indicated in Fig. 6a. The deviation with respect to the central line can be explained due to fluctuations of the laser beam within the time it takes to scan each diffracted spot including the measurement for each spot size associated with each diffracted spot. M^2 was calculated by measuring the nine spots displayed on the screen. The results of these measurements are plotted in Fig. 4c, where the white diamond marks represent the beam radius for each diffracted spot, and the solid line represents the theoretical simulation for our real laser beam. In order to check the validity of our results, we did comparative measurements using a conventional technique, where a camera was scanned through the focus of the beam taking a series of measurements sequentially. The results are plotted in Fig. 6b, where the filled circle marks represent the beam radius' obtained by the scanning technique. The best fit for our experimental and simulated measurements gives us the M^2 value of 18.3 and 19.0 using both techniques, the cross-distorted grating and the conventional scanning arrangement, respectively.

5. Conclusions

We design and achieve a compact device for measuring the beam quality for high power laser beams, based on diffractive optics. Our unique design for the proposed diffractive optical element is based on a distorted diffraction grating, specifically a dual crossed-off-axis Fresnel zone plate, placed in close proximity to a focusing lens. This grating setup produces spot diffracted orders images spots which overlaps several object planes into a single image plane. The performance of this technique was verified numerically and experimentally. A standard technique was used to compare the results

obtained with our proposed technique. The comparative results obtained by this method are in good agreement with the standard technique. This technique offers the possibility of being applied in measuring pulse-to-pulse laser beam quality in real time monitoring.

Acknowledgments

The author wishes to acknowledge the support received from The Institute of Physics at Heriot-Watt University in Scotland, especially Professor Dr. D. Hand, for comments and discussions making this letter possible.

*. Correspondence to: e-mail: rcortes@cicese.mx, Phone +52 81 8348 3088.

1. Dieter Schuocker, *High Lasers and Their Industrial Applications* (SPIE Proceedings, vol. 650, 1986).
2. W. Steen, *Manuf. Eng.* **73** (1994) 214.
3. P. Hand Duncan and J.D.C. Jones, *Appl. Opt.* **37** (1998) 1602.
4. Lei Hong and Li Lijun, *Opt. Laser Technol.* **31** (1999) 531.
5. R. Martínez-Herrero, P.M. Mejías, N. Hodgson, and H. Weber, *IEEE J. Quantum Electron.* **31** (1995) 2173.
6. D. Su, A.A.P. Boechat, and J.D.C. Jones, *Opt. Lasers Eng.* **20** (1994) 193.

7. A. Khun *et al.*, *Opt. Lasers Eng.* **34** (2000) 273.

8. D.R. Hall and P.E. Jackson, *The physics and technology of lasers resonators*. (Bristol, Adam Higler, 1989).
9. P.M. Blanchard, D.J. Fisher, S.C. Woods, and A.H. Greenaway, *Appl. Opt.* **39** (2000) 6649.
10. P.M. Blanchard and A.H. Greenaway, *Opt. Commun.* **183** (2000) 29.
11. Blanchard P.M. and A.H. Greenaway, *Appl. Opt.* **32** (1999) 6692.